Full title: Antagonistic paralogs control a switch between growth and pathogen resistance in *C. elegans*

Short title: A switch for *C. elegans* resistance to diverse natural pathogens

Kirthi C. Reddy*, Tal Dror*, Ryan S. Underwood*, Guled A. Osman#, Christopher A. Desjardins^, Christina A. Cuomo^, Michalis Barkoulas#, and Emily R. Troemel*

*Division of Biological Sciences, University of California, San Diego, La Jolla, CA 92093 USA

^Infectious Disease and Microbiome Program, Broad Institute, Cambridge MA 02142 USA

Department of Life Sciences, Imperial College, London SW7 2AZ, UK

Lead contact: Emily Troemel, 9500 Gilman Dr #0349, La Jolla, CA 92093, USA

etroemel@ucsd.edu

Abstract

Immune genes are under intense pressure from pathogens, which cause these genes to diversify over evolutionary time and become species-specific. Through a forward genetic screen we recently described a *C. elegans*-specific gene called *pals-22* to be a repressor of "Intracellular Pathogen Response" or IPR genes. Here we describe *pals-25*, which, like *pals-22*, is a species-specific gene of unknown biochemical function. We identified *pals-25* in a screen for suppression of *pals-22* mutant phenotypes and found that mutations in *pals-25* suppress all known phenotypes caused by mutations in *pals-22*. These phenotypes include increased IPR gene expression, thermotolerance, and immunity against natural pathogens. Mutations in *pals-25* also reverse the reduced lifespan and slowed growth of *pals-22* mutants. Transcriptome analysis indicates that *pals-22* and *pals-25* control expression of genes induced not only by natural pathogens of the intestine, but also by natural pathogens of the epidermis. Indeed, in an independent forward genetic screen we identified *pals-22* as a repressor and *pals-25* as an activator of epidermal defense gene expression. These phenotypic and evolutionary features of *pals-22* and *pals-25* are strikingly similar to species-specific R gene pairs in plants that control immunity against co-evolved pathogens.

Introduction

Evolutionarily ancient genes control core processes in diverse organisms. For example, the >500 million-year-old Hox gene cluster is required for establishing body plan polarity in animals as diverse as worms, flies and humans [1]. However, evolutionarily young genes can also play key roles in development. For example, the *Drosophila* Umbrea gene only evolved within the *Drosophila* lineage in the last 15 million years but is

essential for chromosome segregation in *Drosophila melanogaster* [2]. In general, the functions of evolutionarily young genes are less well understood than the function of evolutionarily ancient genes.

New genes can arise through gene duplication and diversification [3]. Extensive gene duplication can lead to large, expanded gene families, which appear 'species-specific' if there is significant diversification away from the ancestral gene. The function of species-specific genes can provide insight into the pressures imposed upon organisms in their recent evolutionary past. Pathogen infection imposes some of the strongest selective pressure on organisms, and accordingly, many species-specific, expanded gene families are involved in immunity. One example is the family of mouse Naip genes, which encode sensor proteins in the inflammasome that detect bacteria to trigger cytokine release and cell death [4]. Another example is the plant R genes, which detect virulence factors from co-evolved pathogens to activate effector-triggered immunity [5]. Interestingly, a growing theme in plant R genes is that they can function as opposing gene pairs, with one R gene promoting host defense and the other R gene inhibiting host defense. Of note, both the Naip and R genes were identified through unbiased forward genetic screens for immune genes.

Recently, we described a forward genetic screen in *C. elegans* for genes that regulate the transcriptional response to natural intracellular pathogens [6]. From this screen we identified a *C. elegans*-specific gene called *pals-22* that regulates expression of Intracellular Pathogen Response or IPR genes. Interestingly, we found that *pals-22* also regulates proteostasis, potentially through ubiquitin ligase activity (see below). The '*pals*' signature stands for protein containing ALS2CR12 signature, which is found in the single

pals gene in humans called ALS2CR12. A genome-wide association study implicated ALS2CR12 in amyotrophic lateral sclerosis (ALS) [7], although this gene has no known role in ALS, and its biological function is unknown. The *pals* gene family has only a single member each in the mouse and human genomes, but is substantially expanded in *Caenorhabditis* genomes: *C. elegans* has 39 *pals* genes; *C. remanei* has 18 *pals* genes; *C. brenneri* has 8 *pals* genes; and *C. briggsae* has 8 *pals* genes [8].

pals-22 mutants have several striking phenotypes in *C. elegans*. First, *pals-22* mutants have constitutive expression of several IPR genes including the cullin gene *cul-6*, which is predicted to encode a component of a Cullin-Ring Ligase complex. Second, *pals-22* mutants have increased tolerance of proteotoxic stressors, and this increased tolerance requires the wild-type function of *cul-6*. Third, *pals-22* mutants have less robust health in the absence of stressors. In particular, they have slowed development and shorter lifespans compared to wild-type animals. Fourth, as shown by another group who identified *pals-22* in an independent forward genetic screen, *pals-22* mutants have increased transgene silencing, and increased RNA interference (RNAi) against exogenous RNA [8]. Thus, loss-of-function mutations in *pals-22* appear to broadly reprogram the physiology of *C. elegans*.

Here we describe a forward genetic screen for suppressors of *pals-22* and identify another *pals* gene called *pals-25*. Interestingly, although it appears that *pals-25* and *pals-22* are in an operon together, these two genes function antagonistically and direct opposing phenotypes. We show that mutations in *pals-25* strongly suppress all the physiological phenotypes seen in *pals-22* mutants, including IPR gene expression, stress resistance, lifespan, development and transgene silencing. Furthermore, we find

that *pals-22* mutants have increased resistance against natural intracellular pathogens, like the microsporidian species *Nematocida parisii* and the Orsay virus. This increased resistance is suppressed by mutations in *pals-25*. Also, we use RNA-seq analysis to show that the *pals-22/pals-25* gene pair (hereafter referred to as *pals-22/25*) regulate expression of a majority of the genes induced by natural pathogens of the intestine and find that most of these genes are also induced by blockade of the proteasome. Interestingly, we observe that *pals-22* and *pals-25* also regulate expression of genes induced by natural eukaryotic pathogens infecting through the epidermis. Indeed, in an independent forward genetic screen to find regulators of epidermal defense gene expression we identified additional mutant alleles of *pals-22* and *pals-25*. In summary, the species-specific *pals-22/25* gene pair control an entire physiological program that balances growth with increased proteostasis capacity and resistance against diverse natural pathogens.

Results

pals-25 is required for increased IPR gene expression in *pals-22* mutants

Previously we found that wild-type *pals-22* represses expression of IPR genes: *pals-22* mutants have constitutive expression of several IPR genes including *pals-5* [6]. A transcriptional reporter consisting of the 1273 bp upstream region of *pals-5* fused to GFP, *pals-5p::GFP,* is a reliable marker of IPR gene expression [9] and exhibits strong GFP expression in a *pals-22* mutant background [6] (Fig 1A-C). To find positive regulators of IPR gene expression, we mutagenized *pals-22*; *pals-5p::GFP* strains and screened for loss of GFP expression in F2 animals. From one screen in the *pals-22(jy1)* mutant background and one screen in the *pals-22(jy3)* mutant background we screened a total of ~23,000 haploid genomes and found eight independent mutant alleles that

almost entirely reverse the increased *pals-5p::GFP* expression back to wild-type levels in *pals-22* mutants (Fig 1A-F). All of these alleles are recessive, segregate in Mendelian ratios, and fail to complement each other. These results suggest they all have loss-of-function mutations in the same gene.

Fig 1. *pals-25* is required for increased *pals-5p::GFP* expression in *pals-22* mutants.

(A-E) Mutants isolated from *pals-22* suppressor screens show decreased expression of the *pals-5p::GFP* reporter. Shown are (A) wild-type, (B) *pals-22(jy1)*, (C) *pals-22(jy3)*, (D) *pals-22(jy1) pals-25(jy11)*, and (E) *pals-22(jy3) pals-25(jy9)* animals. Green is *pals-5p::GFP*, red is *myo-2p::mCherry* expression in the pharynx as a marker for presence of the transgene. Images are overlays of green, red and Nomarski channels and were taken with the same camera exposure for all. Scale bar, 100 μm. (F) *pals-5p::GFP* expression quantified in *pals-22* suppressor mutants using a COPAS Biosort machine to measure the mean GFP signal and length of individual animals, indicated by green dots. Mean signal of the population is indicated by black bars, with error bars as SD. Graph is a compilation of three independent replicates, with at least 100 animals analyzed in each replicate. *** $p < 0.001$ with Student's t-test. (G) *pals-22* and *pals-25* gene coding structure (UTR not shown), with blue exons for *pals-22* and red exons for *pals-25*. See S1 Table for residues altered. (H) *pals-5p::GFP* expression in animals treated with either L4440 RNAi control or *pals-25* RNAi, quantified using a COPAS Biosort machine to measure the mean GFP signal and length of animals. Parameters the same as in (F).

We used whole-genome sequencing of two mutant strains (*jy9* and *jy100*) to identify the causative alleles [10] and found predicted loss of function mutations in *pals-25* in both

144 strains. Further sequencing identified *pals-25* mutations in the remaining six mutant
145 strains (Fig 1G, S1 Table). *pals-25* appears to be in an operon just downstream of *pals-*
146 *22*, and while these two genes are paralogs, they share limited sequence similarity, with
147 no significant similarity on the DNA level and only 19.4% identity on the amino acid level.
148 Of note, neither *pals-22* nor *pals-25* have obvious orthologs in other *Caenorhabditis*
149 species, and thus appear to be specific to *C. elegans* [8]. To further confirm that *pals-25*
150 regulates *pals-5p::GFP* gene expression in *pals-22* mutants, we performed RNAi against
151 *pals-25* in a *pals-22*; *pals-5p::GFP* strain. As expected, we found lowered expression of
152 *pals-5p::GFP* (Fig 1H, S2 Fig), indicating that wild-type *pals-25* is required for the
153 increased expression of *pals-5p::GFP* seen in a *pals-22* mutant background.
154
155 These observations suggest that *pals-25* acts downstream of *pals-22* to activate mRNA
156 expression of IPR genes. To test this hypothesis, we used qRT-PCR to measure levels
157 of endogenous mRNA in *pals-22 pals-25* mutants compared to *pals-22* mutants and
158 wild-type animals (Fig 2A). We analyzed mRNA levels of *pals-5*, as well as seven other
159 IPR genes including nematode-specific genes of unknown function (F26F2.1, F26F2.3,
160 and F26F2.4), and predicted ubiquitin ligase components *skr-3, skr-4, skr-5* and *cul-6*.
161 Here we found that mutations in *pals-25* reverse the elevated mRNA levels of all eight of
162 these IPR genes in a *pals-22* mutant background back to near wild-type levels.
163 Importantly, a non-IPR gene, *skr-1*, is not affected by mutations in *pals-22* or *pals-25*.
164 These results indicate that in a *pals-22* mutant background, wild-type *pals-25* activates
165 IPR gene expression.
166
167 **Fig 2. *pals-25* is required for increased IPR gene expression in *pals-22* mutants,**
168 **but not for IPR induction in response to infection or proteasome inhibition.**

(A) qRT-PCR measurement of gene expression in *pals-22* and *pals-22 pals-25* animals, shown as the fold change relative to wild-type control. (B-C) qRT-PCR measurement of IPR gene expression in *pals-22(jy3)* and *pals-22(jy3) pals-25(jy9)* animals following 4 hours of infection with *N. parisii* (B) or treatment with the proteasome inhibitor bortezomib (C). For (A-C), results shown are the average of two independent biological replicates and error bars are SD. * $p < 0.05$ with Student's t-test.

Previous analysis indicated that *pals-22* is broadly expressed in several tissues in the animal, including the intestine and the epidermis [6, 8]. Similarly, we found that *pals-25* is broadly expressed. Using a fosmid containing *pals-25* with endogenous *cis* regulatory control and tagged at the C terminus with GFP and 3xFLAG [11], we observed PALS-25::GFP expression throughout the animal, including expression in the neurons, epidermis, and intestine (S2B Fig). We did not see any change in PALS-25::GFP expression after *pals-22* RNAi treatment (S2C Fig).

IPR genes are induced by infection and by proteasome blockade in *pals-22 pals-25* mutants

As *pals-25* is required to activate IPR gene expression in a *pals-22* mutant background, we wondered whether *pals-25* was required for inducing IPR gene expression in response to external triggers. We originally identified IPR genes because of their induction by *N. parisii* infection [6, 9], which is an intracellular pathogen in the Microsporidia phylum that invades and undergoes its entire replicative life cycle inside *C. elegans* intestinal cells [12]. We therefore infected animals with *N. parisii* and compared induction of IPR genes in *pals-22 pals-25* mutants and wild-type animals at 4 hours (Fig 2B). Here we found similar levels of IPR gene induction in *pals-22 pals-25* and wild-type

194 animals, suggesting that *pals-22/25* regulate expression of IPR genes in parallel to
195 infection. Next, we examined the role of *pals-22/25* in the transcriptional response to
196 proteasome blockade, which is another trigger of IPR gene expression [9] (Fig 2C). We
197 used bortezomib, which is a small molecule inhibitor of the 26S proteasome. Here again,
198 we found that bortezomib treatment induced IPR gene expression in *pals-22 pals-25*
199 mutants at levels similar to wild-type animals. Therefore *pals-22/25* appear to regulate
200 IPR gene expression in parallel to infection and proteasomal stress.
201
202 ***pals-25* mutations reverse multiple physiological phenotypes caused by *pals-22***
203 **mutations**
204 *pals-22* mutants have several striking physiological phenotypes, including slowed growth
205 and shorter lifespans, as well as increased resistance to proteotoxic stress like heat
206 shock [6]. Therefore, we investigated whether mutations in *pals-25* suppress these
207 phenotypes of *pals-22* mutants. First, we investigated developmental rate by measuring
208 the fraction of animals that reach the fourth larval (L4) stage by 48 hours after
209 embryogenesis. Nearly all wild-type animals are L4 at this timepoint, whereas less than
210 20% of *pals-22* mutants are L4 (Fig 3A). We found that mutations in *pals-25* completely
211 reverse this delayed development of *pals-22* mutants, with nearly all *pals-22 pals-25*
212 mutants reaching the L4 stage by 48 hours (Fig 3A). Next, we analyzed lifespan, as
213 previous work showed that *pals-22* mutants have a significantly shortened lifespan
214 compared to wild-type animals [6, 8]. Here again we found that *pals-25* mutations
215 reversed this effect, with *pals-22 pals-25* mutants having lifespans comparable to wild-
216 type animals (Fig 3B, S3A-B Fig). Next, we investigated the effect of *pals-25* mutations
217 on the thermotolerance capacity of *pals-22* mutants, which is greatly enhanced
218 compared to wild-type animals. We found that *pals-22 pals-25* double mutants have

survival after heat shock at levels similar to wild-type animals (Fig 3C, S3C-D Fig), indicating that *pals-25* is required for the enhanced thermotolerance of *pals-22* mutants. Thus, these results show that in a *pals-22* mutant background, wild-type *pals-25* is required to delay development, shorten lifespan and enhance thermotolerance.

Fig 3. *pals-25* mutations suppress diverse phenotypes of *pals-22* mutants. (A) *pals-25* mutation suppresses the developmental delay of *pals-22* mutants. Fraction of animals reaching the L4 larval stage 48 hours after eggs were laid is indicated. Results shown are the average of three independent biological replicates, with 100 animals assayed in each replicate. Error bars are SD. *** $p < 0.001$ with Student's t-test. (B) Lifespan of wild type, *pals-22(jy3)*, and *pals-22(jy3) pals-25(jy9)* animals. Assays were performed with 40 animals per plate, and three plates per strain per experiment. This experiment was repeated three independent times with similar results, with data from a representative experiment shown. See Figures S2A and S2B for other replicates. p-value for *pals-22(jy3)* compared to *pals-22(jy3) pals-25(jy9)* is <0.0001 using the Log-rank test. (C) The increased survival of *pals-22* mutants after heat shock is suppressed by mutations of *pals-25*. Animals were incubated for 2 hours at 37°C followed by 24 hours at 20°C, and then assessed for survival. Strains were tested in triplicate, with at least 30 animals per plate. Mean fraction alive indicates the average survival among the triplicates, errors bars are SD. ** $p < 0.01$. Assay was repeated three independent times with similar results, and data from a representative experiment are shown. See Figures S2C and S2D for other replicates. (D-I) *pals-25* mutation suppresses transgene silencing in *pals-22* mutants. (D) *ric-19p::GFP* expression quantified in *pals-22* and *pals-22 pals-25* mutants using a COPAS Biosort machine to measure the mean GFP signal and length of individual animals, indicated by green dots. Mean signal of the population is

indicated by black bars with error bars as SD. Graph is a compilation of three independent replicates, with at least 100 animals analyzed in each replicate. *** $p < 0.001$ with Student's t-test. In (E-I), green is neuronal expression of *ric-19p::GFP*. Shown are (E) wild-type, (F) *pals-22(jy1)*, (G) *pals-22(jy3)*, (H) *pals-22(jy1) pals-25(jy11)*, and (I) *pals-22(jy3) pals-25(jy9)* animals. Images are overlays of green and Nomarski channels and were taken with the same camera exposure for all. Scale bar, 100 μm.

Previous work from the Hobert lab identified *pals-22* in a screen for regulators of reporter gene expression in neurons [8]. They found that mutations in *pals-22* led to decreased levels of GFP reporter expression in neurons and other tissues, and wild-type *pals-22* thus acts as an 'anti-silencing' factor of multi-copy transgene expression. Therefore, we analyzed the effects of *pals-25* mutations on transgene silencing in *pals-22* mutants. Here we found that *pals-25* mutations reverse the enhanced silencing of a neuronally expressed GFP transgene in *pals-22* mutants (Fig 3D-I), indicating that wild-type *pals-25* activity is required to silence expression from multi-copy transgenes in a *pals-22* mutant background. Of note, previous work found that a *pals-25* mutation alone does not affect transgene silencing [8]. In summary, mutations in *pals-25* appear to fully reverse all previously described phenotypes of *pals-22* mutants.

pals-22 mutants have immunity against coevolved intestinal pathogens of the intestine, which is suppressed by _pals-25_ mutations

In addition to the previously described phenotypes of *pals-22* mentioned above, we analyzed resistance of these mutants to intracellular infection. First we analyzed the resistance of *pals-22* mutants to *N. parisii* infection. We fed animals a defined dose of microsporidia spores and measured pathogen load inside intestinal cells. We analyzed

pathogen load at 30 hours post infection (hpi), when *N. parisii* is growing intracellularly in the replicative meront stage, and found greatly lowered pathogen load in *pals-22* mutants compared to wild-type animals (Fig 4A-F). We then tested *pals-22 pals-25* double mutants and found these animals to have resistance comparable to wild-type. One explanation for the altered levels of *N. parisii* observed in the intestines of *pals-22* mutant animals is that these mutants have lowered feeding or accumulation of pathogen in the intestine, and thus simply have a lower exposure to *N. parisii*. To address this concern, we added fluorescent beads to our *N. parisii* infection assay and measured accumulation in the intestinal lumen. Here we found that *pals-22* mutants and *pals-22 pals-25* double mutants accumulated fluorescent beads at comparable levels to wild-type animals (S4A Fig), suggesting that their pathogen resistance to *N. parisii* is not simply due to lowered exposure to the pathogen in the intestinal lumen. As a positive control in this assay we tested *eat-2(ad465)* mutants and found that they had reduced fluorescent bead accumulation, consistent with their previously characterized feeding defect [13]. Altogether, these results indicate that *pals-22* and *pals-25* regulate resistance to infection by microsporidia.

Figure 4. *pals-22* mutants have increased resistance to infection by *N. parisii* or Orsay virus, dependent on *pals-25*.

(A-E) Images of (A) wild-type, (B) *pals-22(jy1)*, (C) *pals-22(jy3)*, (D) *pals-22(jy1) pals-25(jy11)*, and (E) *pals-22(jy3) pals-25(jy9)* animals infected with *N. parisii* as L1s, fixed 30 hours post infection, and stained by FISH with an *N. parisii*-specific probe (red). Scale bar, 100 μm. (F) *N. parisii* FISH signal quantified using a COPAS Biosort machine to measure the mean red signal and length of individual animals, indicated by red dots. Mean signal of the population is indicated by black bars, with error bars as SD. Graph is

294 a compilation of three independent replicates, with at least 100 animals analyzed in each
295 replicate. *** $p < 0.001$ with Student's t-test. (G) Fraction of animals infected with the
296 Orsay virus 18 hours post infection is indicated. Animals were fixed and stained by FISH
297 with a virus-specific probe, and scored visually for infection. Results shown are the
298 average of three independent biological replicates, with 100 animals assayed in each
299 replicate. Error bars are SD. *** $p < 0.001$ with Student's t-test. (H-L) Images of (H) wild-
300 type, (I) *pals-22(jy1)*, (J) *pals-22(jy3)*, (K) *pals-22(jy1) pals-25(jy11)*, and (L) *pals-22(jy3)*
301 *pals-25(jy9)* animals infected with the Orsay virus as L1s, fixed 18 hours post infection,
302 and stained by FISH with a virus-specific probe (red). Scale bar, 100 μm. (M)
303 Quantification of dsRed fluorescence levels in wild-type, *pals-22*, and *pals-22 pals-25*
304 animals after 16 hours of exposure to dsRed-expressing PA14. Red fluorescence was
305 measured using a COPAS Biosort machine to measure the mean red signal and length
306 of individual animals, indicated by red dots. Mean signal of the population is indicated by
307 black bars, with error bars as SD. Graph is a compilation of three replicates, with at least
308 100 animals analyzed in each replicate. *** $p < 0.001$ with Student's t-test.
309
310 We also investigated resistance of *pals-22* mutants and *pals-22 pals-25* double mutants
311 to other pathogens. First, we measured resistance to infection by the Orsay virus. Like
312 *N. parisii*, Orsay virus is a natural pathogen of *C. elegans,* and replicates inside of *C.*
313 *elegans* intestinal cells [14]. We used FISH staining of Orsay viral RNA to quantify the
314 fraction of worms infected at 18 hpi. Here we found that *pals-22* mutants had significantly
315 decreased viral load when compared to wild-type animals (Fig 4G-L). This lowered viral
316 infection in *pals-22* mutants was fully reversed in *pals-22 pals-25* mutants back to wild-
317 type levels. Importantly, we confirmed that *pals-22* and *pals-22 pals-25* mutants do not
318 have altered fluorescent bead accumulation in the intestine compared to wild-type

319 animals in the presence of virus (S4B Fig), indicating that their lowered viral load is not
320 likely due to lowered exposure to the virus.
321
322 Interestingly, we found that *pals-22* mutants did not have reduced pathogen loads when
323 infected with the Gram-negative bacterial pathogen *Pseudomonas aeruginosa* (clinical
324 isolate PA14) (Fig 4M). In fact, these mutants had increased pathogen load, which was
325 suppressed by mutations in *pals-25*. To our knowledge *P. aeruginosa* species are not
326 common pathogens of nematodes in the wild, although under laboratory conditions, *P.*
327 *aeruginosa* PA14 does accumulate in the *C. elegans* intestinal lumen and causes a
328 lethal infection [15]. In summary *pals-22* mutants have increased resistance to natural
329 pathogens of the intestine, but increased susceptibility to PA14, a 'non-natural' pathogen
330 of the intestine.
331
332 **RNA-seq analysis of *pals-22/25*-upregulated genes define the IPR**
333 Previous work indicated that *N. parisii* and the Orsay virus induce a common set of
334 genes, despite these being very different pathogens [9]. We called eight of these genes
335 the IPR subset [6], and here we show they are regulated by *pals-22/25* (Fig 2A). To
336 identify additional genes regulated by *pals-22/25*, we performed RNA-seq analysis of
337 *pals-22* mutants, *pals-22 pals-25* mutants, and wild-type animals. We performed
338 differential gene expression analysis using a FDR<0.01 cutoff (see Materials and
339 Methods for a complete description of criteria) and determined that 2,756 genes were
340 upregulated in *pals-22* mutants compared to wild-type animals (Fig 5A, S7 Table). Next
341 we compared *pals-22* mutants to *pals-22 pals-25* double mutants and found that 744
342 genes were upregulated (Fig 5A, S7 Table). Of these two comparisons, there are 702
343 genes in common that are upregulated both in *pals-22* mutants compared to wild-type

344 animals and in *pals-22* mutants compared to *pals-22 pals-25* double mutants (Fig 5A).
345 Therefore, these 702 genes are negatively regulated by wild-type *pals-22* and require
346 the activity of the wild-type *pals-25* for their induction in the absence of *pals-22.* These
347 702 genes include genes like our *pals-5* reporter (Fig 1) and other IPR genes (Fig 2).
348
349 **Fig 5. The *pals-22/25* gene pair transcriptionally regulates genes that are induced**
350 **by *N. parisii* infection or proteasome blockade**
351 (A) Venn diagram comparing 1) genes upregulated in *pals-22* mutants compared to wild-
352 type animals, 2) genes upregulated in *pals-22* mutants compared to *pals-22 pals-25*
353 double mutants and 3) genes induced in wild-type animals in response to *N. parisii*
354 infection. Gene sets 1 and 2 were obtained from RNA-seq data outlined in this study,
355 and Gene set 3 was obtained via RNA-seq in a previous study [9]. We define the IPR
356 genes as the 80 genes common across the three gene sets. (B-D) The relative mRNA
357 levels measured by RNA-seq in: *pals-22(jy3)* animals compared to wild-type; *pals-*
358 *22(jy3) pals-25(jy9)* animals compared to wild-type; and wild-type animals treated with
359 the proteasome inhibitor bortezomib (BTZ) compared to DMSO (vehicle control for BTZ).
360 * FDR<0.01 as calculated by edgeR and limma (see Materials and Methods) indicates
361 the gene is considered to be differentially expressed. (B) *pals* genes induced by *N.*
362 *parisii* infection are also regulated by *pals-22/25* and induced by BTZ. (C) Species-
363 specific F26F2 genes are regulated by the *pals-22/25* gene pair and are induced by BTZ.
364 (D) The Cullin-Ring Ligase components Cullin (*cul)* and Skp-related (*skr)* genes that are
365 upregulated during *N. parisii* infection are also regulated by the *pals-22/25* gene pair and
366 induced by BTZ. (E) Venn Diagram showing overlap between: IPR genes defined in (A);
367 genes upregulated by treatment with BTZ; and genes upregulated due to *skn-1* RNAi
368 [16]. See Tables S2 and S3 for detailed expression levels of genes discussed here.

We next compared these 702 *pals-22/25* regulated genes to genes induced during *N. parisii* infection identified in a previous study [9] to expand our list of IPR genes. Out of 127 genes induced during *N. parisii* infection we found that the *pals-22/25* gene pair regulated mRNA expression of 80 of these genes (Fig 5A). Specifically, of the 25 *pals* genes induced upon intracellular infection, all are induced in *pals-22* mutants and reverted back to wild-type levels in *pals-22 pals-25* double mutants (Fig 5B, S7 Table). Notably, all *pals* genes that are not regulated by *pals-22/25* are also not induced by infection. Furthermore, the other nematode-specific genes F26F2.1, F26F2.3, and F26F2.4, which are induced by *N. parisii* and Orsay virus infection, were also found to be induced in *pals-22* mutants and brought back to wild-type levels in *pals-22 pals-25* double mutants (Fig 5C). In addition, we found that the ubiquitin ligase components are similarly regulated (Fig 5D). These studies thus define IPR genes as the 80 genes that are: 1) induced by *N. parisii* infection, 2) induced in a *pals-22* mutant background, and 3) reversed back to wild-type levels in *pals-22 pals-25* double mutants.

Genes regulated by *pals-22/25* and infection are also regulated by proteasomal stress

Previous work indicated that blockade of the proteasome, either pharmacologically or genetically, will induce expression of a subset of IPR genes [9]. To determine the IPR genes that are induced by proteasome stress, we performed RNA-seq analysis to define the whole-genome response to this stress. Again, we conducted differential expression analysis and compared gene expression of animals after 4 hours of exposure to the proteasome inhibitor bortezomib compared to the DMSO vehicle control. From these experiments we determined that 988 genes are induced following bortezomib treatment,

using the cut-off mentioned above and described in the Materials and Methods. Interestingly, nearly all of the IPR genes described above are also induced following bortezomib treatment (Fig 5E). Previous work has shown that genes induced by *N. parisii* do not include the proteasome subunits induced by proteasome blockade as part of the bounceback response [9]. The bounceback response is induced via the transcription factor SKN-1. Consistent with these results, here we find that the IPR genes induced by bortezomib are distinct from those regulated by the transcription factor SKN-1, as defined by a previous study [16]. The overlap between SKN-1 regulated genes and IPR genes includes only one gene (Fig 5E).

As shown earlier, *pals-22* mutants have increased resistance to heat shock, and previous work indicated that there is overlap between genes induced by chronic heat stress and genes induced by *N. parisii* and virus infection [9]. However, the genes in common are distinct from the canonical chaperones, or Heat Shock Proteins (HSPs), which are induced by the heat shock transcription factor HSF-1. To learn more about the connection between heat shock response, HSF-1, and the IPR, we compared the IPR genes with those induced by HSF-1 as defined in a previous study [17]. Here we found 8 genes in common between our set of 80 IPR genes and the set of 368 genes upregulated by HSF-1, none of which are predicted to encode chaperone proteins (S10 Table). We also compared the 368 genes upregulated by HSF-1 with the 702 genes that are regulated by *pals-22/25* and found 59 genes in common (S10 Table). These genes include secreted C-type lectins and F-box genes, but do not include chaperones. In summary, HSF-1 regulates 59 genes in common with those regulated by *pals-22/25*, but only 8 of these are IPR genes.

pals-22 **and** ***pals-25*** **regulate expression of genes induced by other natural pathogens**

Next, we used Gene Set Enrichment Analysis (GSEA) to broadly compare *pals-22/25*-regulated genes to genes regulated by other pathogens, stressors, and stress-related pathways. Here we found that *pals-22/25* does not significantly regulate expression of genes induced by the Gram-negative bacterial pathogen *P. aeruginosa* or the Gram-positive bacterial pathogens *Staphylococcus aureus* and *Enterococcus faecalis* as analyzed in previous studies (Fig 6). Notably, the strains used in these studies are clinical isolates. Furthermore, these pathogen species are not known to be natural pathogens of nematodes and are not found inside *C. elegans* intestinal cells before there is extensive tissue damage in the host [18]. (Refer to S9 Table for additional comparisons among genes regulated by *pals-22/25*, bortezomib treatment, and other pathogens and stress pathways.)

Fig 6. Functional analysis of genes transcriptionally regulated by the *pals-22/25* gene pair

Correlation of genes transcriptionally regulated by the *pals-22/25* gene pair and genes differentially expressed due to bortezomib treatment with genes that are up- or downregulated in response to infection by pathogens or other environmental stresses. Analysis was performed using the GSEA 3.0 software package (see Materials and Methods) and correlation is quantified as a Normalized Enrichment Score (NES). A positive NES (yellow) indicates correlation with upregulated genes in the denoted comparison while a negative NES (blue) indicates correlation with downregulated genes. Black cells indicate no significant correlation was detected, a FDR>0.25, or p>0.05).

443 *FDR<0.05. For more detailed results, see S9 Table. For details on the gene sets used
444 see S8 Table.
445
446 Because *pals-22* and *pals-25* regulate expression of a majority of the genes induced by
447 natural intestinal pathogens like *N. parisii* and the Orsay virus, we investigated whether
448 they regulate the transcriptional response to natural pathogens that infect other tissues.
449 The fungal pathogen *Drechmeria coniospora* infects and penetrates the epidermis of
450 nematodes, triggering a GPCR signaling pathway that upregulates expression of
451 neuropeptide-like (*nlp*) genes including *nlp-29* to promote defense [15]. Our
452 transcriptome analysis shows that *pals-22/25* regulate a significant number of genes in
453 common with *Drechmeria* infection (S10 Table). Notably these genes do not include the
454 well-characterized neuropeptide *nlp* defense genes, although they do include many of
455 the *pals* genes. A more recently described natural pathogen of *C. elegans* is
456 *Myzocytiopsis humicola,* which is an oomycete that also infects through the epidermis
457 and causes a lethal infection [19]. Here as well, *pals-22/25* regulate a significant number
458 of genes in common with those induced by *M. humicola* infection, including the chitinase-
459 like '*chil'* genes that promote defense against this pathogen (S10 Table). Interestingly,
460 these *chil* genes, like the *pals* genes, are species-specific [8, 19].
461
462 We next used Ortholist [20] to determine which genes identified from our RNA-seq
463 analyses have predicted human orthologs. Of the 702 genes regulated by *pals-22/25,*
464 279 genes (39.7%) have predicted human orthologs (S11 Table). In contrast, of the 368
465 genes induced in *hsf-1* mutants 190 (51.6%) have predicted human orthologs.
466 Therefore, more of the genes regulated by the conserved transcription factor *hsf-1* have
467 human orthologs compared to genes regulated by the *C. elegans*-specific *pals-22/25*

gene pair. Furthermore, when we restrict our analysis to just the 80 IPR genes, only 14 (17.5%) have predicted human orthologs, indicating that the transcriptional response to natural infection is enriched for genes that are not well-conserved.

***pals-22/25* control expression of epidermal defense genes induced by oomycetes**

As described above, the RNA-seq analysis of genes regulated by *pals-22/25* indicated that this gene pair controls expression of genes induced by diverse natural pathogens of *C. elegans*. Indeed, in a forward genetic screen for *C. elegans* genes that regulate expression of the *M. humicola*-induced *chil-27p::GFP* reporter, we isolated independent loss-of-function alleles of *pals-22* (Fig 7A). These mutant alleles cause constitutive expression of *chil-27p::GFP* in the epidermis in the absence of infection (Fig 7B). RNAi against *pals-22* also led to constitutive GFP expression (S12 Fig), in a manner that is indistinguishable from that observed upon infection with *M. humicola*. These results indicate that *pals-22* acts as a negative regulator of *chil-27* expression in the epidermis.

Fig 7. *pals-22* and *pals-25* regulate expression of *chil-27* in the epidermis. (A) *pals-22* and *pals-25* gene coding structure (UTR not shown), with blue exons for *pals-22* and red exons for *pals-25*. See S1 Table for residues altered. (B) Expression of *chil-27p::GFP* is regulated by *pals-22* and *pals-25*. Shown are control, *pals-22(icb88)*, *pals-22(icb90)*, *pals-22(icb90) pals-25(icb91)*, and *pals-22(icb90) pals-25(icb92)* animals. The *col-12p::mCherrry* transgene is constitutively expressed in the epidermis. Scale bar, 100 μm. (C) Relative levels of *chil* gene expression. *pals-22/25* regulate *chil* genes that are induced upon infection by oomycete. *FDR<0.01 as calculated by edgeR and limma (see Materials and Methods) indicates the gene is considered to be differentially expressed.

493

494 We then used a *pals-22; chil-27p::GFP* strain for a suppressor screen, analogous to the
495 one described earlier for suppressors of GFP expression in *pals-22; pals-5p::GFP* (Fig
496 1). Interestingly, in this new screen we isolated two new alleles of *pals-25* which fully
497 suppress the constitutive gene expression of *chil-27p::GFP* seen in *pals-22* mutants (Fig
498 7A-B), indicating that wild-type *pals-25* acts as a positive regulator of *chil-27* expression.
499 These observations are consistent with our differential expression analysis, which
500 determined that *chil-27* is induced in a *pals-22* mutant background and that *pals-25* is
501 required for this induction (Fig 7C). Therefore, *pals-22/25* act as a switch not only for
502 genes induced in the intestine by natural intestinal pathogens, but also as a switch for
503 genes induced in the epidermis by natural epidermal pathogens of *C. elegans*.

504

505 **Discussion**

506 In many organisms, there is a balance between growth and pathogen resistance. In
507 particular, many studies in plants have indicated that genetic immunity to disease comes
508 at a cost to the yield of crops [21]. Here we define a program in *C. elegans* that controls
509 a balance between organismal growth with resistance to natural pathogens, which is
510 regulated by the *pals-22/25* species-specific gene pair. These genes act as a switch
511 between a 'defense program' of enhanced resistance against diverse natural pathogens
512 like microsporidia and virus, improved tolerance of proteotoxic stress and increased
513 defense against exogenous RNA [8], and a 'growth program' of normal development and
514 lifespan (Fig 8). We call this physiological defense program the "IPR" and it appears to
515 be distinct from other canonical stress response pathways in *C. elegans*, including the
516 p38 MAP kinase pathway, the insulin-signaling pathway, and the heat shock response,
517 among others [6]. Our previous analyses indicated that ubiquitin ligases may play a role

518 in executing the IPR program, as the cullin/CUL-6 ubiquitin ligase subunit is required for
519 the enhanced proteostasis capacity of *pals-22* mutants [6].
520
521 **Fig 8. Model for *pals-22/pals-25* regulation of response to natural pathogens of *C.***
522 ***elegans*.**
523
524 *pals-22* mutants are highly resistant to the microsporidian pathogen *N. parisii*, which is
525 the most common parasite found in wild-caught *C. elegans* [22, 23]. Little is known about
526 innate immune pathways that provide defense against *N. parisii*. Canonical immune
527 pathways in *C. elegans* like the p38 MAP kinase pathway provide defense against most
528 pathogens tested in *C. elegans* but do not provide defense against *N. parisii* [12]. The
529 mechanism by which *pals-22/25* regulate resistance to *N. parisii* is not clear. Our RNA-
530 seq analysis demonstrates that *pals-22/25* affect expression of hundreds of genes in the
531 genome. In particular, most of the genes induced by the natural intracellular pathogens
532 Orsay virus and *N. parisii* are controlled by *pals-22* and *pals-25*, although the function of
533 these IPR genes in defense is unknown. Interestingly, we found that *pals-22/25* regulate
534 expression of genes induced not only by natural intestinal pathogens but also of genes
535 induced by natural epidermal pathogens, such as the oomycete species *M. humicola*. *M.*
536 *humicola* induces expression of *chil*-gene family, and genetic analysis shows these
537 genes promote defense against *M. humicola* [19]. Notably, we identified *pals-22/25* in
538 independent forward genetic screens for regulators of *chil-27* and found that they
539 regulate expression of this defense gene in the epidermis. Thus, *pals-22/25* regulate
540 expression of genes induced by diverse natural pathogens.
541

542 While *pals-25* is required to activate IPR gene expression in a *pals-22* mutant
543 background, it is not required for activation of IPR gene expression in response to *N.*
544 *parisii* infection or proteasomal stress. Therefore, *pals-22/25* may not mediate detection
545 of these pathogens, although they might mediate detection and be redundant with other
546 factors. Intriguingly, the *pals-22/25* gene pair share evolutionary and phenotypic features
547 with plant R gene pairs, which serve as sensors for virulence factors delivered into host
548 cells by co-evolved plant pathogens. For example, the *Arabidopsis thaliana* gene pair
549 RRS1 and RPS4 are species-specific, share the same promoter, and direct opposite
550 outcomes, with RRS1 inhibiting and RPS4 promoting 'effector-triggered immunity'
551 against natural pathogens [24, 25]. Similarly, *pals-22* and *pals-25* are species-specific,
552 appear to be in an operon together, and direct opposite physiological outcomes including
553 defense against natural pathogens. RRS1 and RPS4 proteins directly bind to each other,
554 and RRS1 normally inhibit RPS4 function until detection of bacterial virulence factors, at
555 which point RRS1 inhibition is relieved and RPS4 is free to promote pathogen defense,
556 although the steps downstream of RRS1/RPS4 are poorly understood. Although the *pals*
557 genes do not share sequence similarity with the R genes, in this analogy PALS-22 would
558 inhibit PALS-25 and serve as the 'tripwire' to detect virulence factors from natural
559 pathogens and free PALS-25 to promote the IPR defense program. While this model is
560 attractive, it is purely speculative as we currently have no direct evidence that PALS-22
561 detects virulence factors. Identification of such hypothetical virulence factors would be
562 the focus of future studies.
563
564 The molecular events by which *C. elegans* detects infection are poorly understood,
565 although nematodes do appear to use a form of effector-triggered immunity or
566 'surveillance immunity'. Studies with several distinct pathogens have indicated that *C.*

567 *elegans* induces defense gene expression in response to perturbation of core processes
568 like translation and the ubiquitin-proteasome system [26]. For example, studies with *P.*
569 *aeruginosa* demonstrated that *C. elegans* detects the presence of the translation-
570 blocking Exotoxin A through its effects on host translation, not through detection of the
571 shape of the toxin [27, 28]. In addition to this mode of detection, *C. elegans* may also
572 detect specific molecular signatures like canonical Pathogen-Associated Molecular
573 Patterns (PAMPs). In all likelihood, several types of pathogen detection are used by *C.*
574 *elegans*. Surprisingly however, there have been no direct PAMP ligand/receptor
575 interactions demonstrated for pattern recognition receptors (PRR) in the worm, although
576 there has been a Damage-Associated Molecular Pattern (DAMP)/G-protein-coupled
577 receptor interaction demonstrated to be critical for response to *Drechmeria* infection [29].
578 Indeed, *C. elegans* lacks many PRR signaling pathways that are well described in flies
579 and mammals. For example, the *C. elegans* single Toll-like receptor *tol-1* does not act
580 canonically and worms appear to have lost its downstream transcription factor NFkB,
581 which is critical for innate immunity in flies and mammals [30]. Perhaps conservation of
582 immune genes is only reserved for defense against rare, 'non-natural' pathogens,
583 because genes that are important for immunity are subject to attack and inhibition by
584 microbes [31]. Thus, immune genes that provide defense against natural pathogens from
585 the recent evolutionary past will not be broadly conserved but rather will be species-
586 specific, like rapidly evolving R genes in plants. While R genes have been shown to
587 encode proteins that detect virulence factors secreted into host cells by co-evolved plant
588 pathogens, the mechanism by which they activate downstream immune signaling is
589 unclear. We propose that the IPR physiological program regulated by the *pals-22/25*
590 antagonistic paralogs in *C. elegans* could be analogous to effector-triggered immunity

591 regulated by opposing R gene pairs like RRS1/RPS4 used in plants for resistance
592 against co-evolved pathogens.
593
594 Interestingly, an example of vertebrate-specific antagonistic paralogs has recently been
595 described to play a role in regulating nonsense-mediated RNA decay (NMD) [32]. These
596 studies provide a potential explanation to the long-standing question of how gene
597 duplications are retained, when they are presumably redundant immediately following
598 gene duplication. Specifically, this model predicts that gene duplication events can be
599 rapidly retained if the proteins made from these genes are involved in protein-protein
600 interactions. With just one non-synonymous nucleotide change that switches a wild-type
601 copy to become dominant negative within a multimeric signaling complex, a gene
602 duplication event can be selected for and retained in the heterozygote state – i.e. in one
603 generation. Perhaps in this way, new genes can be born and survive, when gene pairs
604 can evolve to direct opposing functions like the Upf3a/3b paralogs in NMD, and the
605 RRS1/RPS4 and *pals-22/25* paralogs in immunity/growth.
606
607
608
609 **Methods**
610 *Strains*
611 *C. elegans* were maintained at 20°C on Nematode Growth Media (NGM) plates seeded
612 with Streptomycin-resistant *E. coli* OP50-1 bacteria according to standard methods [33].
613 We used N2 wild-type animals. Mutant or transgenic strains were backcrossed at least
614 three times. See S1 Table for a list of all strains used in this study.
615

EMS screens and cloning of alleles

pals-22 mutant worms (either the *jy1* or *jy3* allele) carrying the *jyIs8[pals-5p::GFP, myo-2p::mCherry]* transgene were mutagenized with ethyl methane sulfonate (EMS) (Sigma) using standard procedures as described [34]. L4 stage P0 worms were incubated in 47 mM EMS for 4 hours at 20°C. Worms were screened in the F2 generation for decreased expression of GFP using the COPAS Biosort machine (Union Biometrica). Complementation tests were carried out by generating worms heterozygous for two mutant alleles and scoring *pals-5p::GFP* fluorescence. For whole-genome sequencing analysis of mutants, genomic DNA was prepared using a Puregene Core kit (Qiagen) and 20X sequencing coverage was obtained. We identified only one gene (*pals-25*) on LGIII containing variants predicted to alter function in both mutants sequenced (*jy9* and *jy100*). Additional *pals-25* alleles were identified by Sanger sequencing. Screens in the strains carrying the *icbIs4[chil-27p::GFP, col-12p::mCherry]* transgene were performed in a similar manner except that we used 24 mM EMS to recover the *pals-22* alleles (*icb88*, *icb90*) and 17 mM EMS for the *pals-22(icb90)* suppressor screen and that in both cases we selected F2 animals manually using a Zeiss Axio ZoomV16 dissecting scope. The two *pals-22* alleles (*icb88*, *icb90*) were identified by whole genome sequencing of GFP positive F2 recombinants after crossing to the polymorphic isolate CB4856 as previously described [35] whereas the two *pals-25* alleles were found by direct sequencing of the mutant strains. The *pals-22(icb89)* allele was identified by Sanger sequencing. See S1 Table for a list of all mutations identified.

RNA interference

RNA interference was performed using the feeding method. Overnight cultures of RNAi clones in the HT115 bacterial strain were seeded onto NGM plates supplemented with

5mM IPTG and 1mM carbenicillin and incubated at 25°C for 1 day. Eggs from bleached parents or synchronized L1 stage animals were fed RNAi until the L4 stage at 20°C. For all RNAi experiments an *unc-22* clone leading to twitching animals was used as a positive control to test the efficacy of the RNAi plates. The *pals-22* RNAi clone (from the Ahringer RNAi library) was verified by sequencing. The *pals-25* RNAi clone was made with PCR and includes 1079 base pairs spanning the second, third, and fourth exons of *pals-25*. This sequence was amplified from N2 genomic DNA, cloned into the L4440 RNAi vector, and then transformed into HT115 bacteria for feeding RNAi experiments.

Quantitative RT-PCR

Endogenous mRNA expression changes were measured with qRT-PCR as previously described [6]. Synchronized L1 worms were grown on NGM plates at 20°C to the L4 stage and then collected in TriReagent (Molecular Research Center, Inc.) for RNA extraction. For *N. parisii* infection, 7 x 10^6 spores were added to plates with L4 stage worms and then incubated at 25°C for 4 hours before RNA isolation. Bortezomib (or an equivalent amount of DMSO) was added to L4 stage worms for a final concentration of 20 µM; plates were then incubated at 20°C for 4 hours before RNA isolation. At least two independent biological replicates were measured for each condition, and each biological replicate was measured in duplicate and normalized to the *snb-1* control gene, which did not change upon conditions tested. The Pffafl method was used for quantifying data [36].

Heat shock assay

Worms were grown on standard NGM plates until the L4 stage at 20°C and then shifted to 37°C for two hours. Following heat shock, plates were laid in a single layer on the bench top for 30 minutes to recover, and then moved to a 20°C incubator overnight. Worms were scored in a blinded manner for survival 24 hours after heat shock; animals

not pumping or responding to touch were scored as dead. Three plates were assayed for each strain in each replicate, with at least 30 worms per plate, and three independent assays were performed.

GFP fluorescence measurement

Synchronized L1 stage animals were grown at 20°C to the L4 stage. The COPAS Biosort machine (Union Biometrica) was used to measure the time of flight (as a measure of length) and fluorescence of individual worms. At least 100 worms were measured for each strain, and all experiments were repeated three times.

Lifespan

L4 stage worms were transferred to 6 cm NGM plates seeded with OP50-1 bacteria and incubated at 25°C. Worms were scored every day, and animals that did not respond to touch were scored as dead. Animals that died from internal hatching or crawled off the plate were censored. Worms were transferred to new plates every day throughout the reproductive period. Three plates were assayed for each strain in each replicate, with 40 worms per plate.

Microscopy

Worms were anesthetized with 10 µM levamisole in M9 buffer and mounted on 2% agarose pads for imaging. Images in Figure S1B and S1C were captured with a Zeiss LSM700 confocal microscope. All other *C. elegans* images were captured with a Zeiss AxioImager M1 or Axio Zoom.V16.

N. parisii and Orsay virus infection assays

690 *N. parisii* spores were prepared as previously described [37], and Orsay virions were
691 prepared as described previously [9]. For pathogen load analysis, synchronized L1
692 worms were plated with a mixture of OP50 bacteria and 5 x 10^5 *N. parisii* spores or a
693 1:20 dilution of Orsay virus filtrate, and then incubated at 25°C for either 30 hours (*N.*
694 *parisii*) or 18 hours (Orsay virus) before fixing with paraformaldehyde. Fixed worms were
695 stained with individual FISH probes conjugated to the red Cal Fluor 610 dye (Biosearch
696 Technologies) targeting either *N. parisii* ribosomal RNA or Orsay virus RNA. *N. parisii*
697 pathogen load was measured with the COPAS Biosort machine (Union Biometrica).
698 Orsay virus infection was assayed visually using the 10x objective on a Zeiss
699 AxioImager M1 microscope. In feeding measurement assays, plates were set up as for
700 pathogen infection with the addition of fluorescent beads (Fluoresbrite Polychromatic
701 Red Microspheres, Polysciences Inc.). Worms were fixed in paraformaldehyde after 30
702 minutes and red fluorescence signal was measured with the COPAS Biosort machine
703 (Union Biometrica).
704
705 *P. aeruginosa pathogen load*
706 Overnight cultures of a *P. aeruginosa* PA14-dsRed strain [38] were seeded onto SK
707 plates with 50 µg/ml ampicillin, and then incubated at 37°C for 24 hours followed by
708 25°C for 24 hours. Worms at the L4 stage were washed onto the PA14-dsRed plates,
709 incubated at 25°C for 16 hours, and then assayed with a COPAS Biosort machine
710 (Union Biometrica) for the amount of red fluorescence inside each animal.
711
712 *RNA-seq sample preparation*
713 Synchronized L1 stage worms were grown on 10 cm NGM plates seeded with OP50-1
714 *E. coli* at 20°C until worms had reached the L4 stage. N2, *pals-22(jy3)*, and *pals-22(jy3)*

715 *pals-25(jy9)* strains were then shifted to 25°C for 4 hours before harvesting for RNA
716 extraction. Bortezomib (or an equivalent amount of DMSO) was added to plates with L4
717 stage N2 worms for a final concentation of 20uM; plates were then incubated at 20°C for
718 4 hours before RNA isolation. RNA was isolated with TriReagent purification, followed by
719 RNeasy column cleanup (Qiagen), as described [39]. RNA quality was assessed by
720 Tapestation analysis at the Institute for Genomic Medicine (IGM) at UC San Diego.
721 Paired-end sequencing libraries were then constructed with the TruSeq Stranded mRNA
722 method (Illumina), followed by sequencing on HiSeq4000 machine (Illumina).
723
724 *RNA-seq analysis*
725
726 Sequencing reads were aligned to WormBase release WS235 using Bowtie 2 [40], and
727 transcript abundance was estimated using RSEM [41]. Differential expression analysis
728 was performed in RStudio (v1.1.453) [42] using R (v3.50) [43] and Bioconductor (v3.7)
729 [44] packages. As outlined in the RNAseq123 vignette [45], data was imported, filtered
730 and normalized using edgeR [46], and linear modeling and differential expression
731 analysis was performed using limma [47]. An FDR [48] cutoff of <0.01 was used to
732 define differentially expressed genes; no fold-change criteria was used. Lists of
733 upregulated genes used for comparisons were exported and further sanitized to remove
734 dead genes and update WBGeneIDs to Wormbase release WS263.
735
736 *Functional analysis*
737 Functional analysis was performed using Gene Set Enrichment Analysis (GSEA) v3.0
738 software [49, 50]. Normalized RNA-seq expression data were converted into a GSEA-
739 compatible filetype and ranked using the signal-to-noise metric with 1,000 permutations.
740 Gene sets from other studies were converted to WBGeneIDs according to WormBase

741 release WS263. Independent analyses were performed for each of three comparisons:
742 untreated *pals-22(jy3)* versus untreated N2 animals; untreated *pals-22(jy3)* versus
743 untreated *pals-22(jy3) pals-25(jy9)* animals; bortezomib treated N2 versus DMSO vehicle
744 control treated N2. Results were graphed based on their NES-value using GraphPad
745 Prism 7 (GraphPad Software, La Jolla, CA).
746

747 **Acknowledgments**

748 We acknowledge the IGM for RNAseq library construction and sequencing, Corrina
749 Elder, Jessica Sowa, Ivana Sfarcic, and Michael K. Fasseas for technical support, and
750 Vladimir Lazetic, Robert Luallen, Johan Panek, Ivana Sfarcic, Eillen Tecle, Samira Yitiz
751 and Elina Zuniga for comments on the manuscript.
752
753
754
755

756 **References**

757

758 1. Pearson JC, Lemons D, McGinnis W. Modulating Hox gene functions during
759 animal body patterning. Nature Reviews Genetics. 2005;6(12):893.
760 2. Ross BD, Rosin L, Thomae AW, Hiatt MA, Vermaak D, de la Cruz AFA, et al.
761 Stepwise evolution of essential centromere function in a Drosophila neogene.
762 Science. 2013;340(6137):1211-4.
763 3. Joshi RK, Nayak S. Perspectives of genomic diversification and molecular
764 recombination towards R-gene evolution in plants. Physiology and Molecular
765 Biology of Plants. 2013;19(1):1-9.
766 4. von Moltke J, Ayres JS, Kofoed EM, Chavarría-Smith J, Vance RE. Recognition
767 of bacteria by inflammasomes. Annual review of immunology. 2013;31:73-106.
768 5. Li X, Kapos P, Zhang Y. NLRs in plants. Current opinion in immunology.
769 2015;32:114-21.

6. Reddy KC, Dror T, Sowa JN, Panek J, Chen K, Lim ES, et al. An intracellular pathogen response pathway promotes proteostasis in C. elegans. Current Biology. 2017;27(22):3544-53. e5.
7. Hentati A, Bejaoui K, Pericak-Vance MA, Hentati F, Speer MC, Hung W-Y, et al. Linkage of recessive familial amyotrophic lateral sclerosis to chromosome 2q33–q35. Nature genetics. 1994;7(3):425.
8. Leyva-Díaz E, Stefanakis N, Carrera I, Glenwinkel L, Wang G, Driscoll M, et al. Silencing of repetitive DNA is controlled by a member of an unusual Caenorhabditis elegans gene family. Genetics. 2017;207(2):529-45.
9. Bakowski MA, Desjardins CA, Smelkinson MG, Dunbar TA, Lopez-Moyado IF, Rifkin SA, et al. Ubiquitin-mediated response to microsporidia and virus infection in C. elegans. PLoS pathogens. 2014;10(6):e1004200.
10. Zuryn S, Jarriault S, editors. Deep sequencing strategies for mapping and identifying mutations from genetic screens. Worm; 2013: Taylor & Francis.
11. Sarov M, Murray JI, Schanze K, Pozniakovski A, Niu W, Angermann K, et al. A genome-scale resource for in vivo tag-based protein function exploration in C. elegans. Cell. 2012;150(4):855-66.
12. Troemel ER, Félix M-A, Whiteman NK, Barrière A, Ausubel FM. Microsporidia are natural intracellular parasites of the nematode Caenorhabditis elegans. PLoS biology. 2008;6(12):e309.
13. Raizen DM, Lee R, Avery L. Interacting genes required for pharyngeal excitation by motor neuron MC in Caenorhabditis elegans. Genetics. 1995;141(4):1365-82.
14. Félix M-A, Ashe A, Piffaretti J, Wu G, Nuez I, Bélicard T, et al. Natural and experimental infection of Caenorhabditis nematodes by novel viruses related to nodaviruses. PLoS biology. 2011;9(1):e1000586.
15. Kim D, Ewbank J. Signaling in the Immune Response. 2015 Dec 22. WormBook [Internet] http://wwwwormbookorg.1-51.
16. Oliveira RP, Abate JP, Dilks K, Landis J, Ashraf J, Murphy CT, et al. Condition‐adapted stress and longevity gene regulation by Caenorhabditis elegans SKN‐1/Nrf. Aging cell. 2009;8(5):524-41.
17. Li J, Chauve L, Phelps G, Brielmann RM, Morimoto RI. E2F coregulates an essential HSF developmental program that is distinct from the heat-shock response. Genes Dev. 2016;30(18):2062-75. Epub 2016/11/01. doi: 10.1101/gad.283317.116. PubMed PMID: 27688402; PubMed Central PMCID: PMCPMC5066613.
18. Irazoqui JE, Troemel ER, Feinbaum RL, Luhachack LG, Cezairliyan BO, Ausubel FM. Distinct pathogenesis and host responses during infection of C. elegans by P. aeruginosa and S. aureus. PLoS pathogens. 2010;6(7):e1000982.
19. Osman GA, Fasseas MK, Koneru SL, Essmann CL, Kyrou K, Srinivasan MA, et al. Natural infection of C. elegans by an oomycete reveals a new pathogen-specific immune response. Current Biology. 2018;28(4):640-8. e5.
20. Shaye DD, Greenwald I. OrthoList: a compendium of C. elegans genes with human orthologs. PloS one. 2011;6(5):e20085.
21. Ning Y, Liu W, Wang G-L. Balancing Immunity and Yield in Crop Plants. Trends in plant science. 2017.

22. Schulenburg H, Félix M-A. The natural biotic environment of Caenorhabditis elegans. Genetics. 2017;206(1):55-86.
23. Zhang G, Sachse M, Prevost M-C, Luallen RJ, Troemel ER, Félix M-A. A large collection of novel nematode-infecting microsporidia and their diverse interactions with Caenorhabditis elegans and other related nematodes. PLoS pathogens. 2016;12(12):e1006093.
24. Le Roux C, Huet G, Jauneau A, Camborde L, Trémousaygue D, Kraut A, et al. A receptor pair with an integrated decoy converts pathogen disabling of transcription factors to immunity. Cell. 2015;161(5):1074-88.
25. Sarris PF, Duxbury Z, Huh SU, Ma Y, Segonzac C, Sklenar J, et al. A plant immune receptor detects pathogen effectors that target WRKY transcription factors. Cell. 2015;161(5):1089-100.
26. Cohen LB, Troemel ER. Microbial pathogenesis and host defense in the nematode C. elegans. Current opinion in microbiology. 2015;23:94-101.
27. Dunbar TL, Yan Z, Balla KM, Smelkinson MG, Troemel ER. C. elegans detects pathogen-induced translational inhibition to activate immune signaling. Cell host & microbe. 2012;11(4):375-86.
28. McEwan DL, Kirienko NV, Ausubel FM. Host translational inhibition by Pseudomonas aeruginosa Exotoxin A Triggers an immune response in Caenorhabditis elegans. Cell host & microbe. 2012;11(4):364-74.
29. Zugasti O, Bose N, Squiban B, Belougne J, Kurz CL, Schroeder FC, et al. Activation of a G protein-coupled receptor by its endogenous ligand triggers the Caenorhabditis elegans innate immune response. Nature immunology. 2014;15(9):833.
30. Irazoqui JE, Urbach JM, Ausubel FM. Evolution of host innate defence: insights from Caenorhabditis elegans and primitive invertebrates. Nature Reviews Immunology. 2010;10(1):47.
31. Maltez VI, Miao EA. Reassessing the evolutionary importance of inflammasomes. The Journal of Immunology. 2016;196(3):956-62.
32. Shum EY, Jones SH, Shao A, Dumdie J, Krause MD, Chan W-K, et al. The antagonistic gene paralogs Upf3a and Upf3b govern nonsense-mediated RNA decay. Cell. 2016;165(2):382-95.
33. Brenner S. The genetics of Caenorhabditis elegans. Genetics. 1974;77(1):71-94.
34. Kutscher LM, Shaham S. Forward and reverse mutagenesis in C. elegans. WormBook: the online review of C elegans biology. 2014:1.
35. Minevich G, Park DS, Blankenberg D, Poole RJ, Hobert O. CloudMap: a cloud-based pipeline for analysis of mutant genome sequences. Genetics. 2012;192(4):1249-69.
36. Pfaffl MW. A new mathematical model for relative quantification in real-time RT–PCR. Nucleic acids research. 2001;29(9):e45-e.
37. Balla KM, Andersen EC, Kruglyak L, Troemel ER. A wild C. elegans strain has enhanced epithelial immunity to a natural microsporidian parasite. PLoS pathogens. 2015;11(2):e1004583.

38. Djonović S, Urbach JM, Drenkard E, Bush J, Feinbaum R, Ausubel JL, et al. Trehalose biosynthesis promotes Pseudomonas aeruginosa pathogenicity in plants. PLoS pathogens. 2013;9(3):e1003217.
39. Troemel ER, Chu SW, Reinke V, Lee SS, Ausubel FM, Kim DH. p38 MAPK regulates expression of immune response genes and contributes to longevity in C. elegans. PLoS genetics. 2006;2(11):e183.
40. Langmead B, Salzberg SL. Fast gapped-read alignment with Bowtie 2. Nature methods. 2012;9(4):357.
41. Li B, Dewey CN. RSEM: accurate transcript quantification from RNA-Seq data with or without a reference genome. BMC bioinformatics. 2011;12(1):323.
42. Team R. RStudio: integrated development for R. RStudio, Inc, Boston, MA URL http://wwwrstudiocom. 2015.
43. Team RC. R: A language and environment for statistical computing. 2013.
44. Gentleman RC, Carey VJ, Bates DM, Bolstad B, Dettling M, Dudoit S, et al. Bioconductor: open software development for computational biology and bioinformatics. Genome biology. 2004;5(10):R80.
45. Law CW, Alhamdoosh M, Su S, Smyth GK, Ritchie ME. RNA-seq analysis is easy as 1-2-3 with limma, Glimma and edgeR. F1000Research. 2016;5.
46. Robinson MD, McCarthy DJ, Smyth GK. edgeR: a Bioconductor package for differential expression analysis of digital gene expression data. Bioinformatics. 2010;26(1):139-40.
47. Ritchie ME, Phipson B, Wu D, Hu Y, Law CW, Shi W, et al. limma powers differential expression analyses for RNA-sequencing and microarray studies. Nucleic acids research. 2015;43(7):e47-e.
48. Storey JD, Tibshirani R. Statistical significance for genomewide studies. Proceedings of the National Academy of Sciences. 2003;100(16):9440-5.
49. Mootha VK, Lindgren CM, Eriksson K-F, Subramanian A, Sihag S, Lehar J, et al. PGC-1α-responsive genes involved in oxidative phosphorylation are coordinately downregulated in human diabetes. Nature genetics. 2003;34(3):267.
50. Subramanian A, Tamayo P, Mootha VK, Mukherjee S, Ebert BL, Gillette MA, et al. Gene set enrichment analysis: a knowledge-based approach for interpreting genome-wide expression profiles. Proceedings of the National Academy of Sciences. 2005;102(43):15545-50.

Supporting information

S1 Table. Lists of strains and mutations.

S2 Figure. *pals-25* RNAi suppresses increased *pals-5p::GFP* expression in *pals-22* mutants and PALS-25::GFP is expressed broadly.

(A) Wild-type or *pals-22* mutant animals carrying the *pals-5p::GFP* transgene, treated with either L4440 RNAi control or *pals-25* RNAi. Green is *pals-5p::GFP*, red is *myo-2p::mCherry* expression in the pharynx as a marker for presence of the transgene. Images are overlays of green, red, and Nomarski channels and were taken with the same camera exposure for all. Scale bar, 100 μm. (B,C) Confocal fluorescence images of adult animals carrying a fosmid transgene expressing PALS-25::GFP from the endogenous promoter. Animals were treated with either (B) L4440 RNAi control or (C) *pals-22* RNAi. Scale bar, 50 μm.

S3 Figure. *pals-25* mutation suppresses the lifespan and thermotolerance phenotypes of *pals-22* mutants.

(A,B) Lifespan of wild type, *pals-22(jy3)*, and *pals-22(jy3) pals-25(jy9)* animals. Assays were performed with 40 animals per plate, and three plates per strain per experiment. p-value for *pals-22(jy3)* compared to *pals-22(jy3) pals-25(jy9)* is <0.0001 using the Log-rank test. (C,D) Survival of animals after 2 hour heat shock treatment at 37°C followed by 24 hours at 20°C. Strains were tested in triplicate, with at least 30 animals per plate. Mean fraction alive indicates the average survival among the triplicates, errors bars are SD. ** $p < 0.01$, * $p < 0.05$.

S4 Figure. Mutation of *pals-22* or *pals-25* does not affect feeding rates of animals in pathogen infection assays.

(A,B) Quantification of fluorescent bead accumulation in wild-type, *pals-22*, *pals-22 pals-25*, and *eat-2* mutant animals. Beads were mixed with OP50-1 bacteria and either (A) *N.*

923 *parisii* spores or (B) Orsay virus and fed to worms as in infection assays. Worms were
924 fixed in paraformaldehyde after 30 minutes of feeding, and fluorescence of accumulated
925 beads in each animal was measured using a COPAS Biosort machine to measure the
926 mean red signal and length of individual animals, indicated by red dots. Mean signal of
927 the population is indicated by black bars, with error bars as SD. Graph is a compilation of
928 three independent replicates, with at least 100 animals analyzed in each replicate.
929 Statistical analysis was performed using one-way ANOVA. *** $p < 0.001$, ns, not
930 significant.
931
932 **S5 Table. RNA-seq statistics.**
933
934 **S6 Table. FPKM values for all genes in data set.**
935
936 **S7 Table. Differentially expressed genes, as determined by edgeR and limma.**
937
938 **S8 Table. Gene sets used for GSEA and their sources.**
939
940 **S9 Table. Detailed GSEA results.**
941
942 **S10 Table. Gene set overlaps.**
943
944 **S11 Table. Human orthology analysis.**
945
946 **S12 Figure. Induction of *chil-27p::GFP* expression seen after *pals-22* RNAi**
947 **treatment.**

948 Shown are animals treated with either L4440 RNAi control, *pals-22* RNAi, or *M. humicola*

949 infection. The *col-12p::mCherrry* transgene is constitutively expressed in the epidermis.

950 Scale bar, 100 μm.

951

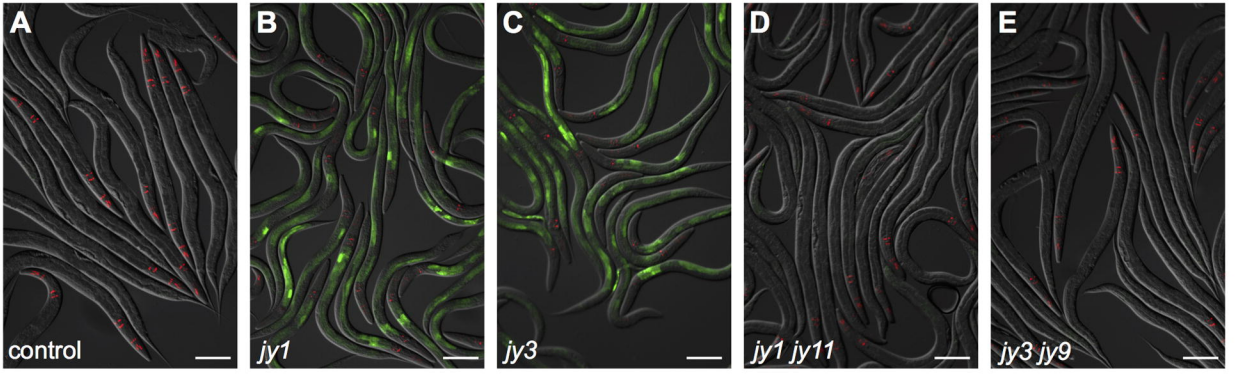
A
control
B
jy1
C
jy3
D
jy1 jy11
E
jy3 jy9

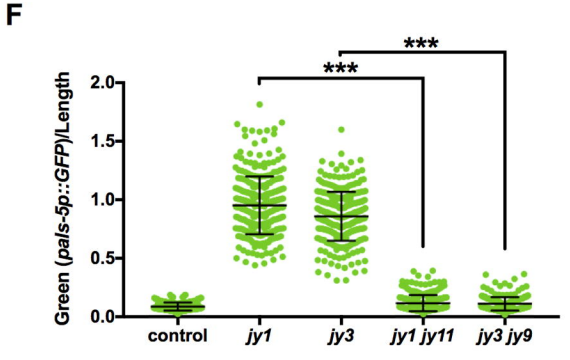
F
Green (pals-5p::GFP)/Length
2.0
1.5
1.0
0.5
0.0
***
***
control
jy1
jy3
jy1 jy11
jy3 jy9

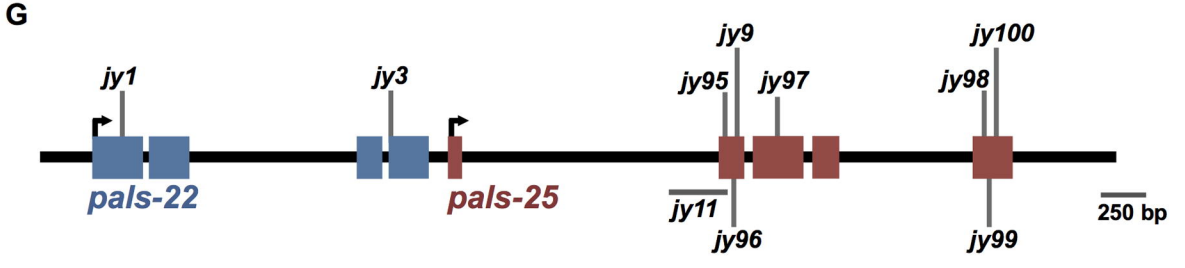
G
jy1
jy3
jy9
jy95
jy97
jy100
jy98
pals-22
pals-25
jy11
jy96
jy99
250 bp

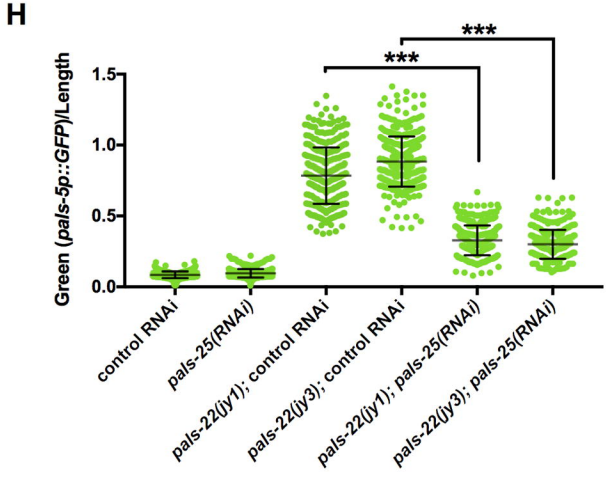
H
Green (pals-5p::GFP)/Length
1.5
1.0
0.5
0.0
***
***
control RNAi
pals-25(RNAi)
pals-22(jy1); control RNAi
pals-22(jy3); control RNAi
pals-22(jy1); pals-25(RNAi)
pals-22(jy3); pals-25(RNAi)

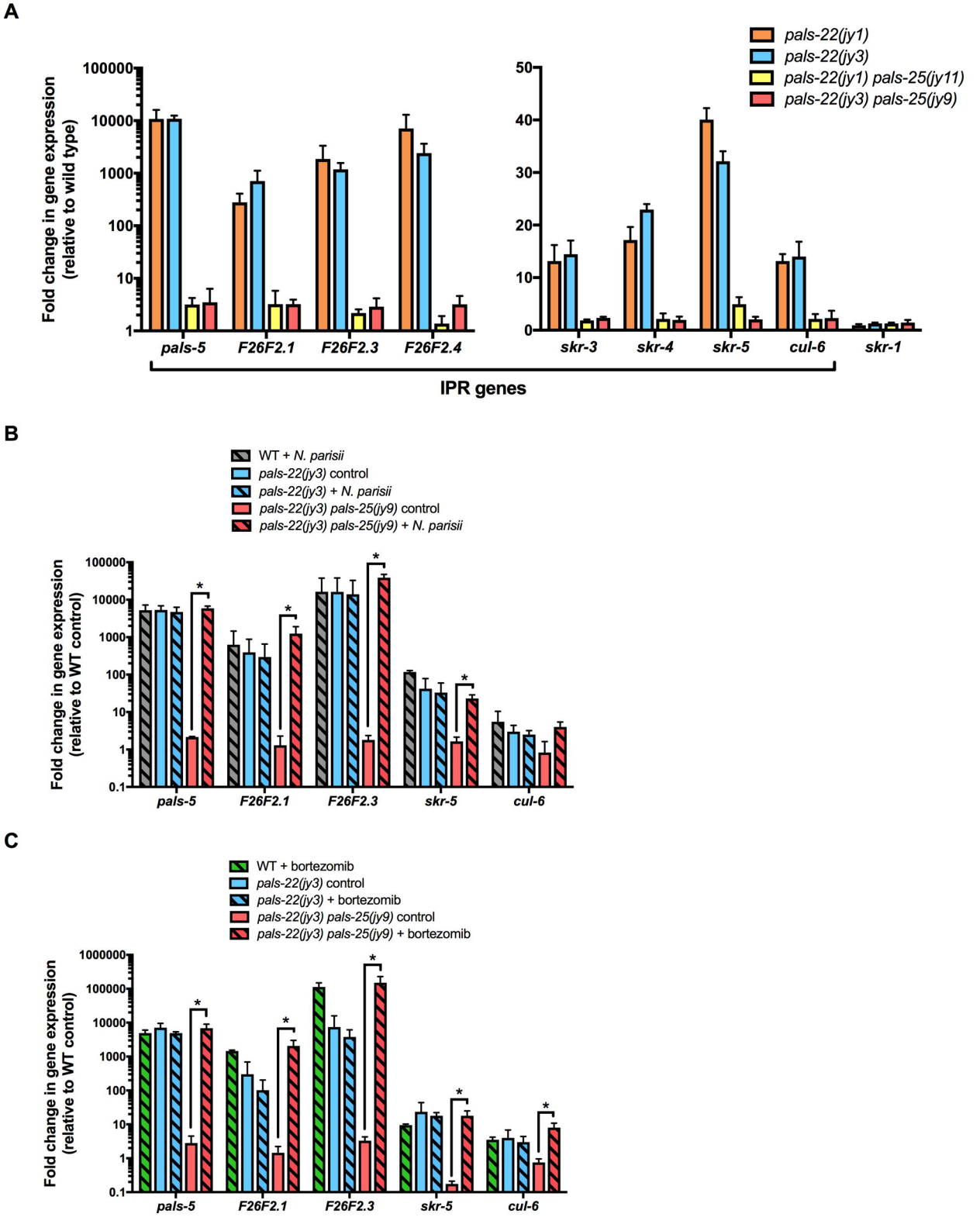
A
pals-22(jy1)
pals-22(jy3)
pals-22(jy1) pals-25(jy11)
pals-22(jy3) pals-25(jy9)
Fold change in gene expression (relative to wild type)
100000
10000
1000
100
10
1
50
40
30
20
10
0
pals-5
F26F2.1
F26F2.3
F26F2.4
skr-3
skr-4
skr-5
cul-6
skr-1
IPR genes
B
WT + N. parisii
pals-22(jy3) control
pals-22(jy3) + N. parisii
pals-22(jy3) pals-25(jy9) control
pals-22(jy3) pals-25(jy9) + N. parisii
Fold change in gene expression (relative to WT control)
100000
10000
1000
100
10
1
0.1
*
pals-5
F26F2.1
F26F2.3
skr-5
cul-6
C
WT + bortezomib
pals-22(jy3) control
pals-22(jy3) + bortezomib
pals-22(jy3) pals-25(jy9) control
pals-22(jy3) pals-25(jy9) + bortezomib
Fold change in gene expression (relative to WT control)
1000000
100000
10000
1000
100
10
1
0.1
*
pals-5
F26F2.1
F26F2.3
skr-5
cul-6

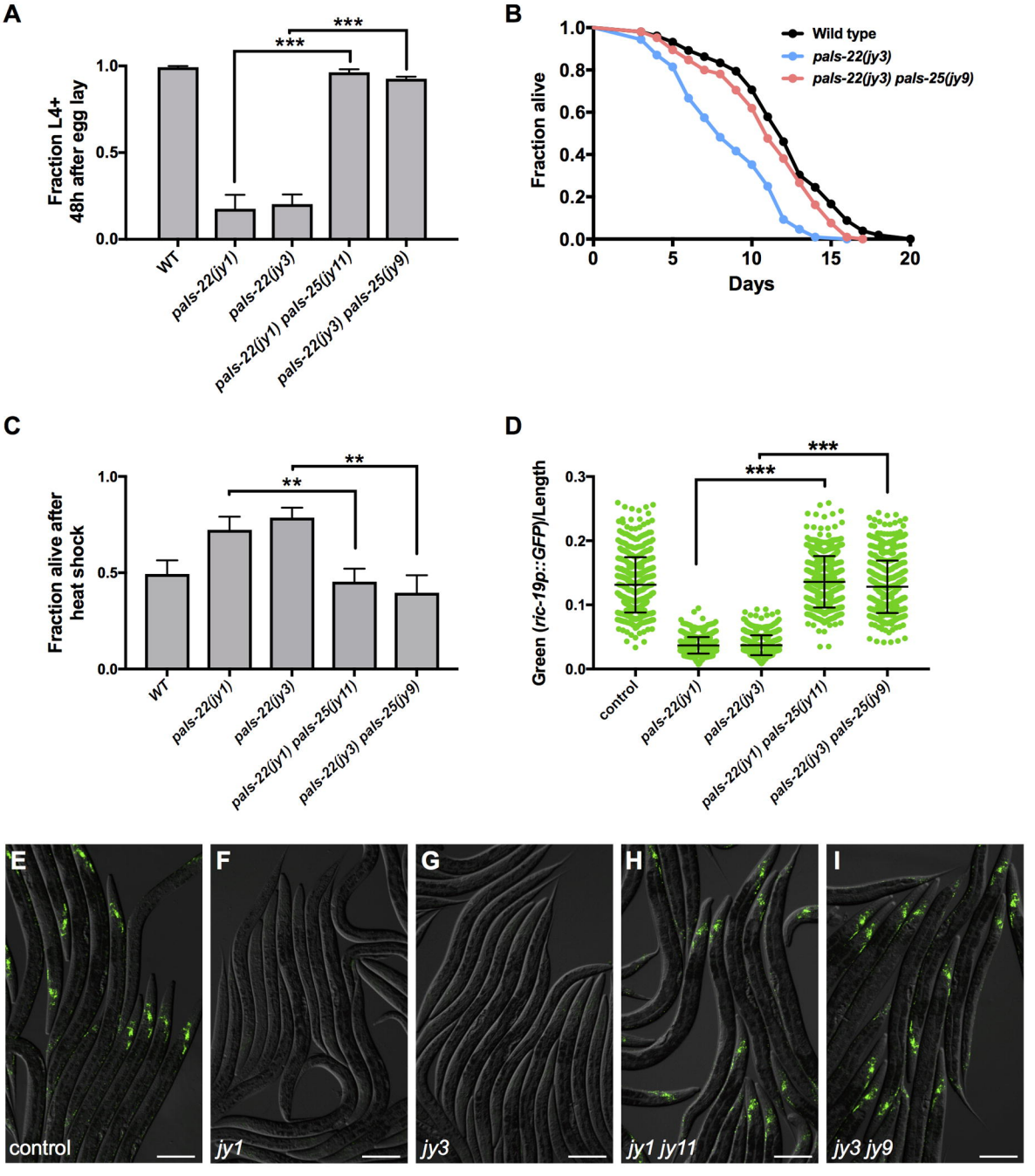
A
Fraction L4+ 48h after egg lay
1.0
0.5
0.0
***
***
WT
pals-22(jy1)
pals-22(jy3)
pals-22(jy1) pals-25(jy11)
pals-22(jy3) pals-25(jy9)
B
Fraction alive
1.0
0.8
0.6
0.4
0.2
0.0
0
5
10
15
20
Days
Wild type
pals-22(jy3)
pals-22(jy3) pals-25(jy9)
C
Fraction alive after heat shock
1.0
0.5
0.0
**
**
WT
pals-22(jy1)
pals-22(jy3)
pals-22(jy1) pals-25(jy11)
pals-22(jy3) pals-25(jy9)
D
Green (ric-19p::GFP)/Length
0.3
0.2
0.1
0.0
***
***
control
pals-22(jy1)
pals-22(jy3)
pals-22(jy1) pals-25(jy11)
pals-22(jy3) pals-25(jy9)
E
control
F
jy1
G
jy3
H
jy1 jy11
I
jy3 jy9

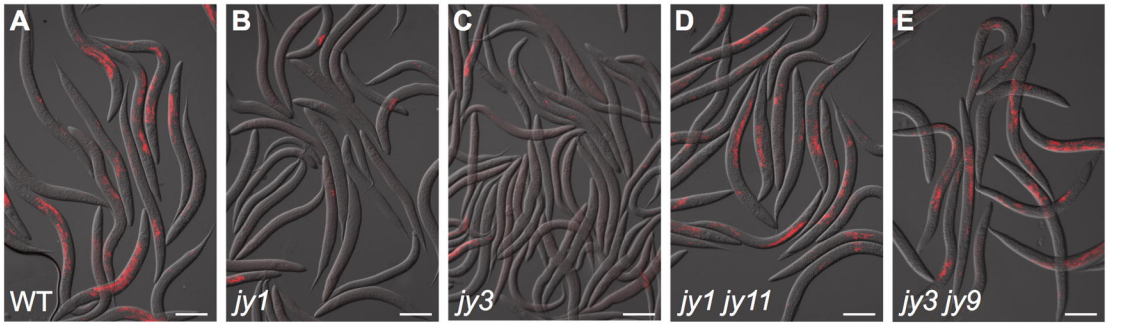
A
WT
B
jy1
C
jy3
D
jy1 jy11
E
jy3 jy9

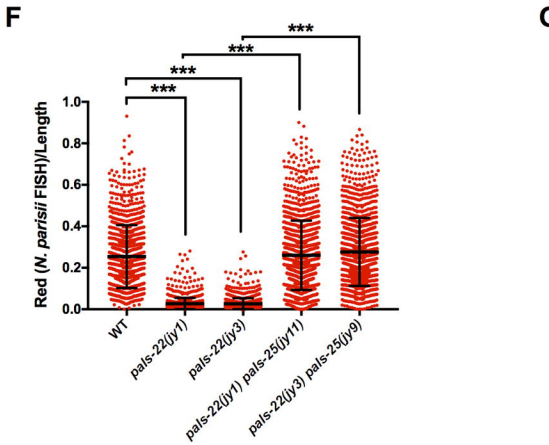
F
Red (N. parisii FISH)/Length
1.0
0.8
0.6
0.4
0.2
0.0
***
***
***
***
WT
pals-22(jy1)
pals-22(jy3)
pals-22(jy1) pals-25(jy11)
pals-22(jy3) pals-25(jy9)

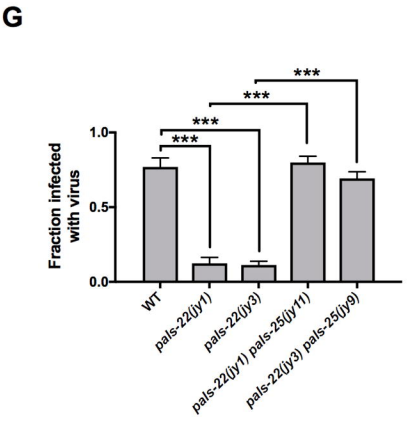
G
Fraction infected with virus
1.0
0.5
0.0
***
***
***
***
WT
pals-22(jy1)
pals-22(jy3)
pals-22(jy1) pals-25(jy11)
pals-22(jy3) pals-25(jy9)

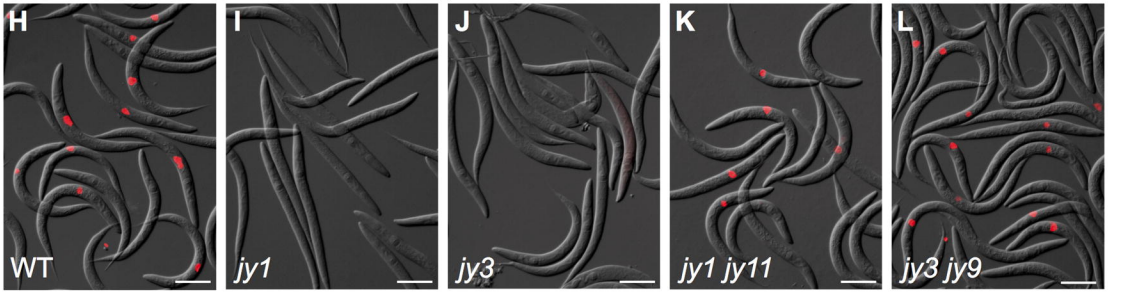
H
WT
I
jy1
J
jy3
K
jy1 jy11
L
jy3 jy9

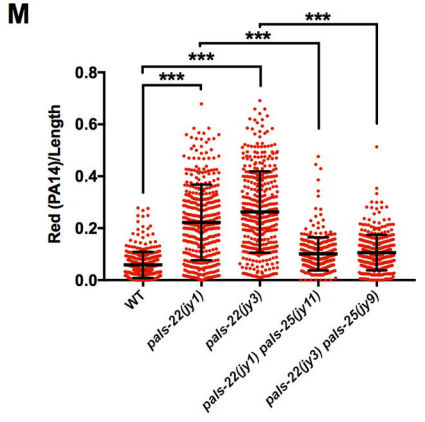
M
Red (PA14)/Length
0.8
0.6
0.4
0.2
0.0
***
***
***
***
WT
pals-22(jy1)
pals-22(jy3)
pals-22(jy1) pals-25(jy11)
pals-22(jy3) pals-25(jy9)

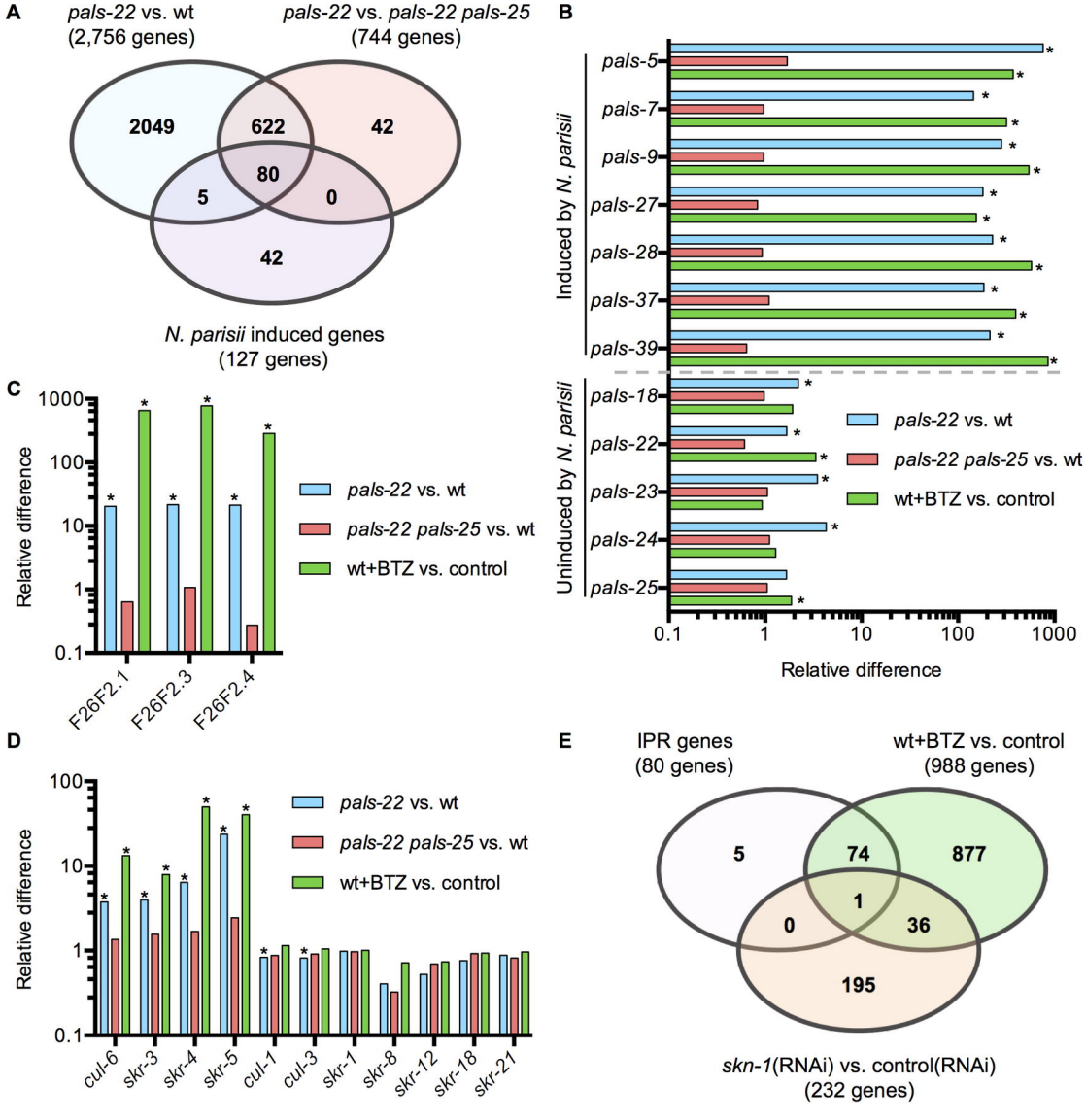
A
pals-22 vs. wt
(2,756 genes)
pals-22 vs. pals-22 pals-25
(744 genes)
2049
622
42
80
5
0
42
N. parisii induced genes
(127 genes)
B
Induced by N. parisii
pals-5
pals-7
pals-9
pals-27
pals-28
pals-37
pals-39
Uninduced by N. parisii
pals-18
pals-22
pals-23
pals-24
pals-25
pals-22 vs. wt
pals-22 pals-25 vs. wt
wt+BTZ vs. control
0.1
1
10
100
1000
Relative difference
C
Relative difference
1000
100
10
1
0.1
F26F2.1
F26F2.3
F26F2.4
pals-22 vs. wt
pals-22 pals-25 vs. wt
wt+BTZ vs. control
D
Relative difference
100
10
1
0.1
cul-6
skr-3
skr-4
skr-5
cul-1
cul-3
skr-1
skr-8
skr-12
skr-18
skr-21
pals-22 vs. wt
pals-22 pals-25 vs. wt
wt+BTZ vs. control
E
IPR genes
(80 genes)
wt+BTZ vs. control
(988 genes)
5
74
877
1
0
36
195
skn-1(RNAi) vs. control(RNAi)
(232 genes)

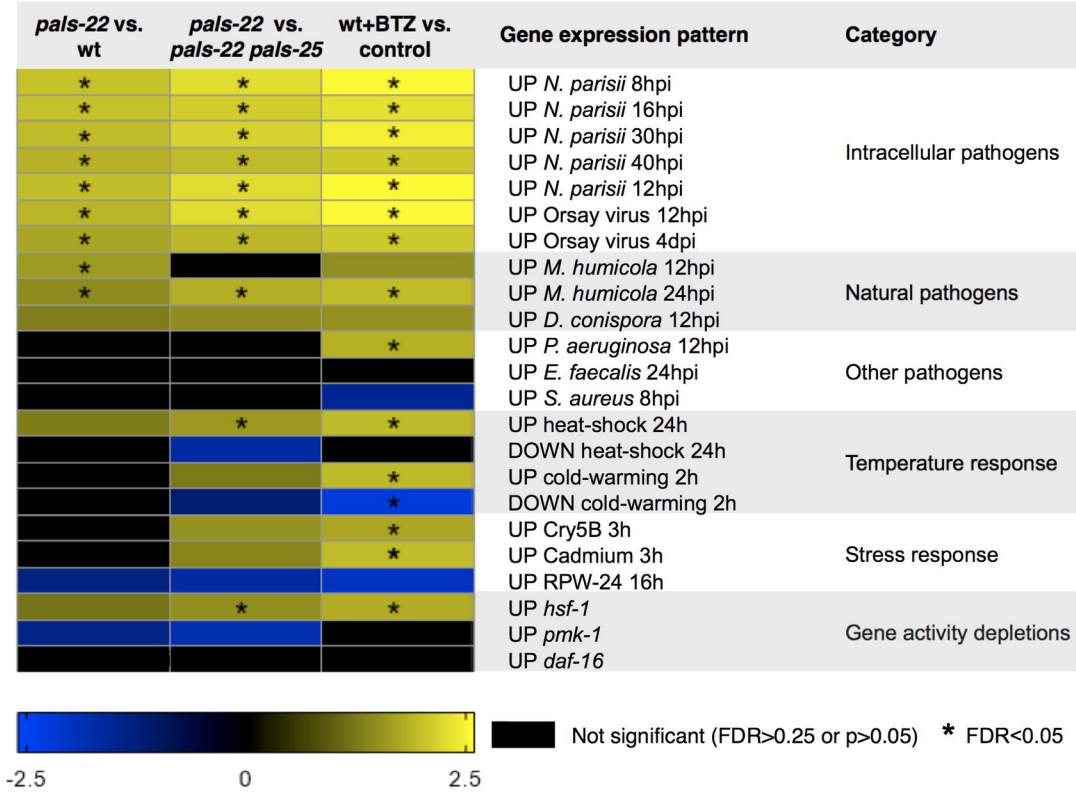
pals-22 vs. wt
pals-22 vs. pals-22 pals-25
wt+BTZ vs. control
Gene expression pattern
Category
UP N. parisii 8hpi
UP N. parisii 16hpi
UP N. parisii 30hpi
UP N. parisii 40hpi
UP N. parisii 12hpi
UP Orsay virus 12hpi
UP Orsay virus 4dpi
Intracellular pathogens
UP M. humicola 12hpi
UP M. humicola 24hpi
UP D. conispora 12hpi
Natural pathogens
UP P. aeruginosa 12hpi
UP E. faecalis 24hpi
UP S. aureus 8hpi
Other pathogens
UP heat-shock 24h
DOWN heat-shock 24h
UP cold-warming 2h
DOWN cold-warming 2h
Temperature response
UP Cry5B 3h
UP Cadmium 3h
UP RPW-24 16h
Stress response
UP hsf-1
UP pmk-1
UP daf-16
Gene activity depletions
-2.5
0
2.5
Not significant (FDR>0.25 or p>0.05)
* FDR<0.05

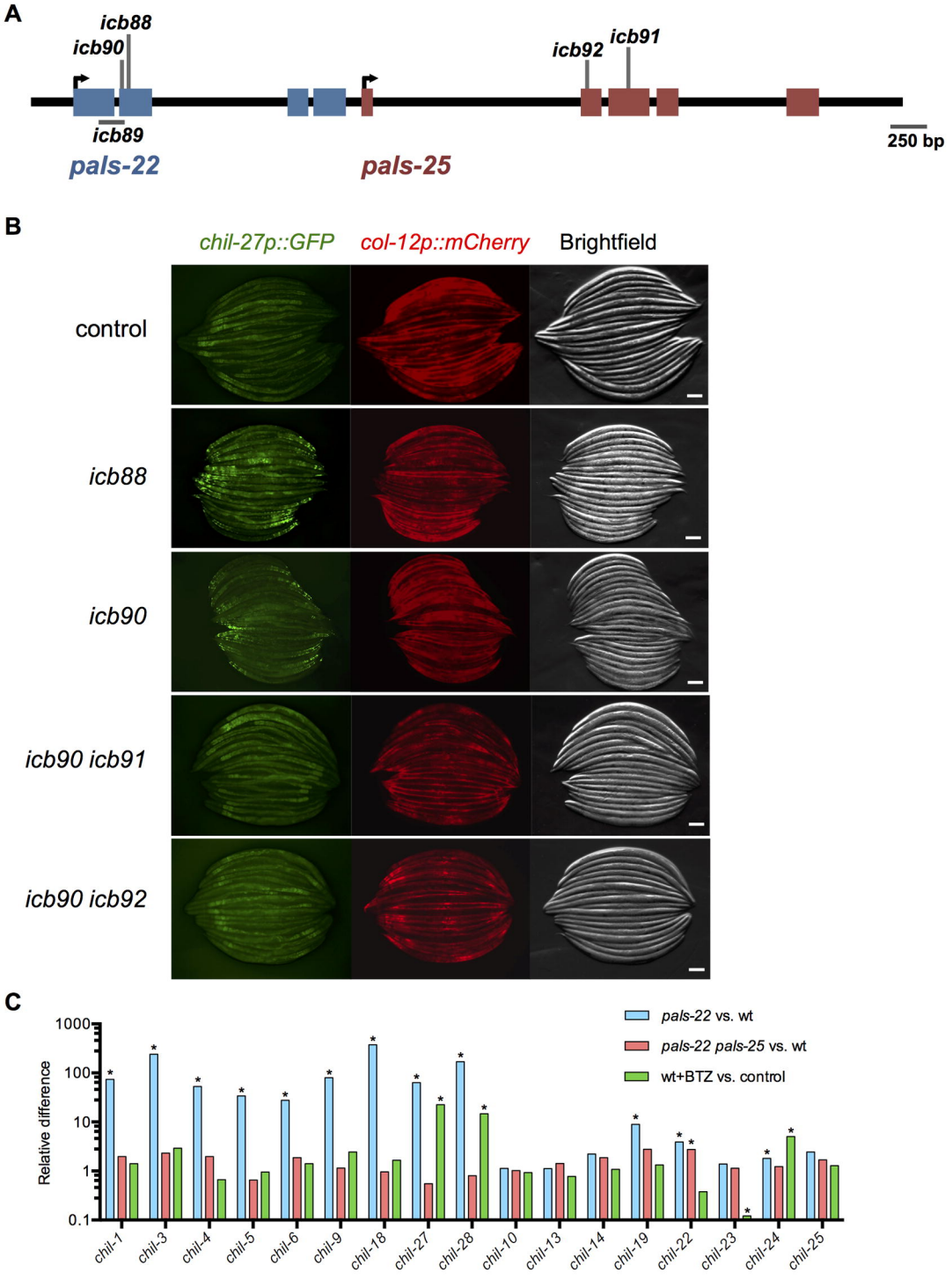
A
icb88
icb90
icb89
pals-22
pals-25
icb92
icb91
250 bp
B
chil-27p::GFP
col-12p::mCherry
Brightfield
control
icb88
icb90
icb90 icb91
icb90 icb92
C
pals-22 vs. wt
pals-22 pals-25 vs. wt
wt+BTZ vs. control
Relative difference
1000
100
10
1
0.1
chil-1
chil-3
chil-4
chil-5
chil-6
chil-9
chil-18
chil-27
chil-28
chil-10
chil-13
chil-14
chil-19
chil-22
chil-23
chil-24
chil-25

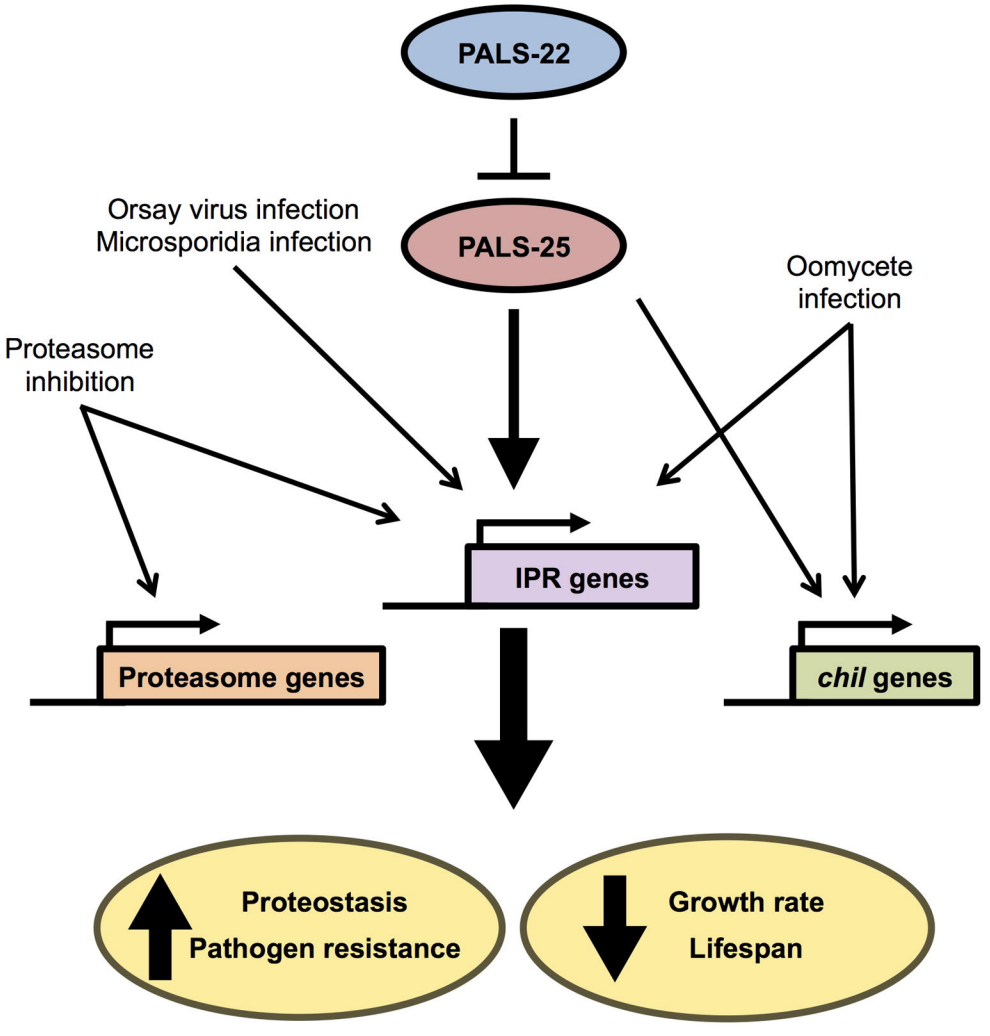
PALS-22
PALS-25
Orsay virus infection
Microsporidia infection
Oomycete
infection
Proteasome
inhibition
IPR genes
Proteasome genes
chil genes
Proteostasis
Pathogen resistance
Growth rate
Lifespan